CrossMark

J. Appl. Prob. **58,** 952–965 (2021)
*doi:*10.1017/jpr.2021.26

ON POINT PROCESSES DEFINED BY ANGULAR CONDITIONS ON DELAUNAY NEIGHBORS IN THE POISSON–VORONOI TESSELLATION

FRANÇOIS BACCELLI,* AND
SANKET S. KALAMKAR,** *INRIA*

Abstract

Consider a homogeneous Poisson point process of the Euclidean plane and its Voronoi tessellation. The present note discusses the properties of two stationary point processes associated with the latter and depending on a parameter θ. The first is the set of points that belong to some one-dimensional facet of the Voronoi tessellation and such that the angle with which they see the two nuclei defining the facet is θ. The main question of interest on this first point process is its intensity. The second point process is that of the intersections of the said tessellation with a straight line having a random orientation. Its intensity is well known. The intersection points almost surely belong to one-dimensional facets. The main question here concerns the Palm distribution of the angle with which the points of this second point process see the two nuclei associated with the facet. We will give answers to these two questions and briefly discuss their practical motivations. We also discuss natural extensions to three dimensions.

Keywords: Stochastic geometry; point process; random polytope; Delaunay graph; Palm calculus; mass transport principle; integral geometry

2010 Mathematics Subject Classification: Primary 60D05
Secondary 52A22; 53C65; 05C80

1. Introduction

The statistical properties of the facets of the Voronoi tessellation of homogeneous point processes of the Euclidean plane are well studied [7].

This note is focused on a question that has apparently not been considered so far, namely the distribution of the angle with which points of the one-dimensional facets of the Poisson–Voronoi tessellation see the two Delaunay neighbors defining the facet. The motivation for this question stems from cellular radio networks and is briefly discussed in this note. The problem is, however, of independent interest. For instance, the analysis leads to expressions for the fraction of one-dimensional (respectively two-dimensional) facets of the typical two-dimensional (respectively three-dimensional) Poisson–Voronoi cell that intersect the Delaunay edge associated with the respective facet.

Received 30 October 2020; revision received 19 February 2021.
* Postal address: INRIA Paris, France, and University of Texas at Austin, USA. Email address: baccelli@math.utexas.edu
** Postal address: INRIA Paris, France.

© The Author(s), 2021. Published by Cambridge University Press on behalf of Applied Probability Trust.

https://doi.org/10.1017/jpr.2021.26 Published online by Cambridge University Press

Let $\Phi = \{X_1, X_2, \ldots\}$ be a homogeneous Poisson point process of intensity $\lambda > 0$ on $\mathbb{R}^2$. Let $\mathcal{V}_{X_i} \in \mathbb{R}^2$ denote the Voronoi cell with nucleus $X_i \in \Phi$:

$$\mathcal{V}_{X_i} := \left\{ x \in \mathbb{R}^2 : \|x - X_i\| \leq \inf_{X_j \in \Phi \setminus \{X_i\}} \|x - X_j\| \right\}.$$

It is well known that the Voronoi cells in question are all a.s. bounded random polygons. The topological boundary of each cell consists of an a.s. finite number of a.s. bounded edges (one-dimensional facets). Each such edge is associated with a so-called Delaunay pair, namely a pair of points of Φ such that the cells of these two points share a common boundary edge.

Consider the set of the points of the one-dimensional facets of the Voronoi tessellation of Φ that see their Delaunay pair with a given angle. This discrete set of points forms a stationary point process. This follows from the fact that it is compatible with the flow of translations that preserves the distribution of the stationary point process Φ [4]. It is discussed in Section 2, where its intensity is determined.

Another natural model features a random line of the plane and the intersections of this line with the one-dimensional facets. This defines a stationary point process on the line, which is discussed in Section 3. The Palm distribution of the angles at which the points of the latter point process see the Delaunay pairs of the facets that intersect the line is determined.

These problems have natural extensions to three dimensions, which are discussed in Section 4.

Finally, Section 5 presents the cellular networking motivations of the problems alluded to above.

2. Planar point process with prescribed Delaunay angle

Below, an intrinsic total order on pairs of points of $\mathbb{R}^2$ is selected, for example the lexicographic order. For all pairs of points (D, D') of $\mathbb{R}^2$ such that $D < D'$ with respect to this order, and for all points Z of $\mathbb{R}^2$, let $\widehat{D, Z, D'}$ denote the angle from D to D' in, for example, the clockwise direction with respect to Z as origin.

Let $\theta \in (0, 2\pi)$ be fixed. For each edge E of the Voronoi tessellation of Φ, there is at most one point Z on this edge satisfying the following property. Let D_1 and D_2 denote the Delaunay neighbors associated with E, ordered as above. Then there is at most one point Z of the edge such that the angle $\widehat{D_1, Z, D_2}$ is equal to $\theta \bmod 2\pi$.

Let Ψ_θ be the point process in $\mathbb{R}^2$ of all points satisfying the above property. This is illustrated in Figure 1, which depicts a point of the edge belonging to the intersection of the boundary of $\mathcal{V}_{X_1}$ and that of $\mathcal{V}_{X_2}$ satisfying this angular property.

Lemma 1. *For all $\theta \in (0, 2\pi)$, Ψ_θ is a stationary and ergodic point process. Its intensity γ_θ is equal to $2\lambda \sin^2(\theta/2)$.*

Proof. For all such θ, Ψ_θ is compatible with the flow of translations preserving the distribution of the point process Φ. It is hence stationary and mixing.

For all ordered points $X_1 \neq X_2$ of Φ, let $Z_\theta(X_1, X_2)$ be the point Z that belongs to the bisector line of (X_1, X_2) and be such that $\widehat{X_1, Z, X_2} = \theta$. Let $B(x, r)$ be the open ball of center x and radius r. The point $Z_\theta(X_1, X_2)$ is in the support of Ψ_θ if and only if $\Phi(B(Z_\theta(X_1, X_2), \|Z_\theta(X_1, X_2) - X_1\|)) = 0$.

https://doi.org/10.1017/jpr.2021.26 Published online by Cambridge University Press

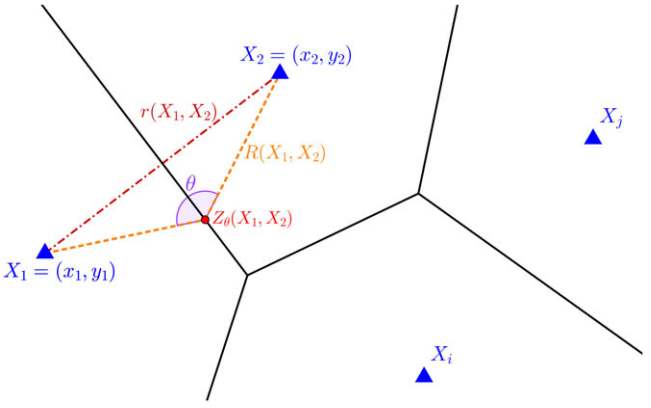


FIGURE 1. Triangles denote the points of the Poisson point process Φ. Solid black lines denote the one-dimensional facets (edges) of the Poisson–Voronoi cells. The point Z_θ is an atom of Ψ_θ, with $\theta \in (0, 2\pi)$ fixed. This is because the angle $X_1, \widehat{Z_\theta, X_2}$ is equal to θ, and the points X_1 and X_2 are the Delaunay neighbors associated with the one-dimensional facet containing Z_θ, with $X_1 < X_2$.

Consider the following mass transport: send mass one from $X \in \Phi$ to $Z \in \Psi_\theta$ if there exists $Y \in \Phi$ such that $Y > X$, $Z = Z_\theta(X, Y)$ (so that $\widehat{X, Z, Y} = \theta$), and $\Phi(B(Z, \|Z - Y\|)) = 0$. Every point of Ψ_θ receives mass one. Hence, by the mass transport principle [1],

$$\begin{aligned}\gamma_\theta &= \lambda \mathbb{P}^0_\Phi[\cup_{Y\in\Phi\setminus\{0\}} \{\Phi(B(Z_\theta(0, Y), \|Z_\theta(0, Y)\|)) = 0\}] \\ &= \lambda \mathbb{E}^0_\Phi\left[\sum_{Y\in\Phi\setminus\{0\}} \mathbf{1}_{\Phi(B(Z_\theta(0,Y),\|Z_\theta(0,Y)\|))=0}\right] \\ &= \lambda \mathbb{E}\left[\sum_{Y\in\Phi} \mathbf{1}_{\Phi(B(Z_\theta(0,Y),\|Z_\theta(0,Y)\|))=0}\right],\end{aligned}$$

where $\mathbb{P}^0_\Phi$ denotes the Palm probability of Φ. The last equality follows from Slivnyak's theorem [3]. Using Campbell's formula [3] first, and then Slivnyak's theorem once more, we obtain

$$\begin{aligned}\mathbb{E}\left[\sum_{Y\in\Phi} \mathbf{1}_{\Phi(B(Z_\theta(0,Y),\|Z_\theta(0,Y)\|))=0}\right] &= \lambda \int_{\mathbb{R}^2} \mathbb{P}^0_\Phi[\Phi(B(Z_\theta(-X, 0), \|Z_\theta(-X, 0)\|)) = 0]\, \mathrm{d}X \\ &= \lambda \int_{\mathbb{R}^2} \mathbb{P}[\Phi(B(Z_\theta(-X, 0), \|Z_\theta(-X, 0)\|)) = 0]\, \mathrm{d}X.\end{aligned}$$

Moving to polar coordinates, we get

$$\gamma_\theta = \pi\lambda^2 \int_0^\infty \exp(-\lambda\pi R^2_{\theta,r})\, r\, \mathrm{d}r,$$

where the integration is only for polar angles from $-\pi/2$ to $\pi/2$ because of the ordering assumption and where $R_{\theta,r} = r/(2\sin(\theta/2))$. It follows that

$$\gamma_\theta = \pi\lambda^2 \int_0^\infty \exp\left(-\lambda\pi \frac{r^2}{4\sin^2(\theta/2)}\right) r\, \mathrm{d}r = 2\lambda \sin^2\frac{\theta}{2}. \qquad \square$$

Here are a few direct corollaries of Lemma 1. The first concerns the mean number of points of Ψ_θ in the typical Voronoi cell.

https://doi.org/10.1017/jpr.2021.26 Published online by Cambridge University Press

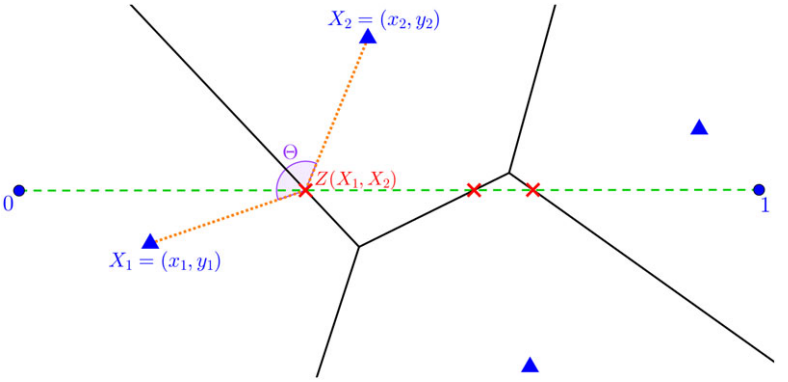


FIGURE 2. Triangles denote the points of Φ. Solid black lines denote the one-dimensional Voronoi facets. A cross denotes a point at the intersection of a Voronoi facet and the x-axis.

Corollary 1.

$$\mathbb{E}^0_\Phi[\Psi_\theta(\mathcal{V}_0)] = 2\sin^2\frac{\theta}{2}.$$

Proof. Consider the following mass transport: send mass one from each point X of Φ to each point of Ψ_θ belonging to $\mathcal{V}_X$. The formula then follows from the mass transport principle. □

The second is as follows.

Corollary 2. *For a two-dimensional Poisson–Voronoi tessellation, the mean number of one-dimensional facets of the typical cell that contain (respectively do not contain) the middle point of the line segment joining the Delaunay neighbors which define the facet is equal to four (respectively two).*

Proof. The result immediately follows from the last corollary and the fact that the mean number of facets of the typical cell is equal to six. □

3. Distribution of Delaunay angle on a line

The setting is the same as above, with Φ a homogeneous Poisson point process of intensity λ on the Euclidean plane.

Consider a straight line with a random orientation and distance to the origin, independent of Φ. The focus below is on the interplay between this line and the Voronoi tessellation of Φ. Thanks to the stationarity and isotropy of Φ, we can assume without loss of generality that this line is the x-axis.

Let $\Upsilon \in \mathbb{R}$ denote the point process of Voronoi boundary crossings along this line. The points of Υ are represented by 'crosses' in Figure 2. This point process is stationary (compatible with shifts along the x-axis). The intensity of the one-dimensional point process Υ is well known to be $\mu = (4\sqrt{\lambda})/\pi$ (see [8]).

Almost surely, each point of Υ belongs to a one-dimensional facet of the Voronoi tessellation of Φ. As such, we can associate with each point Z of Υ the two Delaunay neighbors $X_1(Z)$ and $X_2(Z)$ associated with the one-dimensional facet to which Z belongs. We now define a new order on these points that is slightly different from the earlier order: the points X_1 and X_2 are

https://doi.org/10.1017/jpr.2021.26 Published online by Cambridge University Press

ordered as $X_1 < X_2$ with

$$\Theta(Z) = X_1(\widehat{Z), Z, X_2}(Z) \in (0, 2\pi)$$

such that this angle is computed in a clockwise direction with respect to the straight line. These angles are depicted in Figure 2.

By the same compatibility with respect to shifts along the x-axis, the random variables $\{\Theta(Z)\}$ are marks of the point process Υ. Thus the distribution of Θ under the Palm probability of Υ is well-defined.

Lemma 2. *The distribution of $\Theta = \Theta(0)$ under the Palm probability of Υ has a density equal to*

$$f_\Theta(t) = \frac{1}{4} \sin \frac{t}{2}, \quad 0 < t < 2\pi.$$

Proof. Let t be fixed with $t \in (0, \pi)$. Let Ξ_t^+ denote the thinning of Υ where only points with an angular mark in (t, π) are retained, that is,

$$\Xi_t^+ := \sum_{Z \in \Upsilon} \delta_Z \mathbf{1}_{\Theta(Z) \in (t,\pi)}.$$

Since the selection of points of Υ that are retained to define Ξ_t^+ is based on marks, the point process Ξ_t^+ is also stationary [4]. Let μ_t^+ denote the (linear) intensity of Ξ_t^+. By the definition of Palm probabilities, the two (linear) intensities μ_t^+ and μ are related by the formula $\mu_t^+ = \mu \mathbb{P}_\Upsilon^0(\Theta(0) \in (t, \pi))$, where $\mathbb{P}_\Upsilon^0(\cdot)$ denotes the Palm probability of Υ. Thus

$$\mathbb{P}_\Upsilon^0(\Theta(0) \in (t, \pi)) = \frac{\mu_t^+}{\mu}.$$

For all pairs (X_1, X_2) of ordered points of Φ, let $Z = Z(X_1, X_2)$ denote the intersection of the bisector line of (X_1, X_2) with the x-axis, and let $R = R(X_1, X_2)$ denote the distance between X_1 and $Z(X_1, X_2)$. We have

$$\begin{aligned}\mu_t^+ &= \mathbb{E}\left[\sum_{Z \in \Upsilon} \mathbf{1}_{Z \in [0,1]} \mathbf{1}_{\Theta(Z) \in (t,\pi)}\right] \\ &= \mathbb{E}\left[\sum_{X_1 < X_2 \in \Phi} \mathbf{1}_{Z(X_1,X_2) \in [0,1]} \mathbf{1}_{Z(X_1,X_2) \in \mathcal{V}_{X_1} \cap \mathcal{V}_{X_2}} \mathbf{1}_{X_1, \widehat{Z(X_1,X_2)}, X_2 \in (t,\pi)}\right].\end{aligned}$$

Now using the fact that the factorial moment measure of the Poisson point process of intensity λ is $\lambda^2 \, \mathrm{d}U_1 \, \mathrm{d}U_2$, where $\mathrm{d}U_i$, $i = 1, 2$ represents Lebesgue measure on $\mathbb{R}^2$, we get that for all $t \in (0, \pi)$,

$$\mu_t^+ = \lambda^2 \int_{U_1} \int_{U_2 > U_1} \mathbb{P}_{U_1,U_2}^0(Z(U_1, U_2) \in \mathcal{V}_{U_1} \cap \mathcal{V}_{U_2}) \mathbf{1}_{Z(U_1,U_2) \in [0,1]} \mathbf{1}_{U_1, \widehat{Z(U_1,U_2)}, U_2 \in (t,\pi)} \, \mathrm{d}U_1 \, \mathrm{d}U_2,$$

where $\mathbb{P}_{U_1,U_2}^0$ denotes the two-point Palm probability of Φ. Let $U_1 = (x_1, y_1)$ and $U_2 = (x_2, y_2)$. The coordinates of $Z = Z(U_1, U_2)$ are

$$Z = \left(\frac{1}{2} \frac{(x_2 - x_1)(x_2 + x_1) + (y_2 - y_1)(y_2 + y_1)}{x_2 - x_1}, 0\right).$$

Further, let $R = R(U_1, U_2) = \|U_1 - Z\| = \|U_2 - Z\|$ and $r = \|U_1 - U_2\|$.

https://doi.org/10.1017/jpr.2021.26 Published online by Cambridge University Press

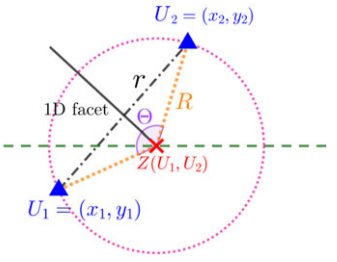


FIGURE 3. The point Z belongs to the one-dimensional facet of U_1 and U_2 if and only if there is no point of Φ within the open disk of radius R that is centered at Z.

Again using the empty ball characterization of the Voronoi cell (see Figure 3), we find that for all $t \in (0, \pi)$

$$\mu_t^+ = \frac{1}{2}\lambda^2 \int_{U_1} \int_{U_2 > U_1} \exp(-\lambda\pi R^2)\mathbf{1}_{2\arcsin\frac{r}{2R} \in (t,\pi)}\mathbf{1}_{Z\in[0,1]}\,\mathrm{d}U_1\,\mathrm{d}U_2,$$

where the $\frac{1}{2}$ comes from mirror symmetry with respect to π and the fact that the integral (without the $\frac{1}{2}$) also counts the points Z with an angle Θ in $(2\pi - t, 2\pi)$. So, for all $t \in (0, \pi)$,

$$\begin{aligned}\mathbb{P}^0_\Upsilon(\Theta(0) \in (t, \pi)) &= \frac{1}{2}\frac{\lambda^2}{\mu} \int_{U_1} \int_{U_2 > U_1} \exp(-\lambda\pi R^2)\mathbf{1}_{2\arcsin\frac{r}{2R} \in (t,\pi)}\mathbf{1}_{Z\in[0,1]}\,\mathrm{d}U_1\,\mathrm{d}U_2 \\ &= \frac{1}{4}\frac{\lambda^2}{\mu} \int_{U_1} \int_{U_2} \exp(-\lambda\pi R^2)\mathbf{1}_{2\arcsin\frac{r}{2R} \in (t,\pi)}\mathbf{1}_{Z\in[0,1]}\,\mathrm{d}U_1\,\mathrm{d}U_2.\end{aligned}$$

The following stretch-rotation transformations are now used:

$$\begin{bmatrix} z_1 \\ z_2 \end{bmatrix} = \begin{bmatrix} 1 & 1 \\ -1 & 1 \end{bmatrix} \begin{bmatrix} x_1 \\ x_2 \end{bmatrix}, \quad \begin{bmatrix} z_3 \\ z_4 \end{bmatrix} = \begin{bmatrix} 1 & 1 \\ -1 & 1 \end{bmatrix} \begin{bmatrix} y_1 \\ y_2 \end{bmatrix}.$$

This yields $\mathrm{d}x_1\,\mathrm{d}x_2\,\mathrm{d}y_1\,\mathrm{d}y_2 = \frac{1}{4}\,\mathrm{d}z_1\,\mathrm{d}z_2\,\mathrm{d}z_3\,\mathrm{d}z_4$. It follows that

$$\begin{aligned}\mathbb{P}^0_\Upsilon(\Theta(0) \in (t, \pi)) = \frac{\lambda^2}{16\mu} \int_{\mathbb{R}^4} &\mathbf{1}_{\frac{1}{2}\left(z_1 + \frac{z_3 z_4}{z_2}\right) \in [0,1]} \\ &\times \mathbf{1}_{2\arcsin\sqrt{\left(z_2^2+z_4^2\right)\Big/\left(z_2^2+z_4^2+z_3^2\left(1+\frac{z_4^2}{z_2^2}\right)\right)} \in (t,\pi)} \\ &\times \mathrm{e}^{-\frac{\lambda\pi}{4}\left(z_2^2+z_4^2+z_3^2\left(1+\frac{z_4^2}{z_2^2}\right)\right)}\,\mathrm{d}z_1\,\mathrm{d}z_2\,\mathrm{d}z_3\,\mathrm{d}z_4.\end{aligned}$$

Now the first indicator function can be eliminated by carrying out the integration over z_1, where the condition for the first indicator function is met when

$$0 \le \frac{1}{2}\left(z_1 + \frac{z_3 z_4}{z_2}\right) \le 1,$$

https://doi.org/10.1017/jpr.2021.26 Published online by Cambridge University Press

or equivalently when

$$-\frac{z_3 z_4}{z_2} \le z_1 \le 2 - \frac{z_3 z_4}{z_2},$$

which yields a factor of two.

Polar coordinates, i.e. $(z_2, z_4) = (r\cos\phi, r\sin\phi)$, are now used to handle the second indicator function:

$$\mathbb{P}^0_\Upsilon(\Theta(0) \in (t,\pi)) = \frac{\lambda^2}{8\mu}\int_{\mathbb{R}} \mathrm{d}z_3 \int_0^\infty r\,\mathrm{d}r \int_0^{2\pi} \mathbf{1}_{2\arcsin \frac{r}{\sqrt{r^2+\frac{z_3^2}{\cos^2\phi}}} \in (t,\pi)} \times \mathrm{e}^{-\frac{\lambda\pi}{4}\left(r^2+\frac{z_3^2}{\cos^2\phi}\right)}\,\mathrm{d}\phi. \tag{1}$$

The next step is to carry out the integration with respect to z_3, which is twice the integral from 0 to ∞.

Since $t < \pi$, the indicator function in the last integral is equal to one on an interval with left limit $z_3^- = 0$ (the argument of the arcsine is one for $z_3 = 0$, so the indicator is equal to one as $t \in (0,\pi)$) and with right limit obtained by solving

$$\frac{r}{\sqrt{r^2 + z_3^2/(\cos^2\phi)}} = \sin\frac{t}{2},$$

namely $z_3^+ = r|\cos\phi|\cot(t/2)$. Hence, for $0 < t < \pi$, we can write (1) as

$$\begin{aligned}
\mathbb{P}^0_\Upsilon(\Theta(0) \in (t,\pi)) &= \frac{\lambda^{3/2}}{4\mu}\int_0^\infty r\,\mathrm{d}r \int_0^{2\pi} |\cos\phi|\,\exp\left(-\frac{\lambda\pi r^2}{4}\right)\mathrm{erf}\left(\frac{r\sqrt{\lambda\pi}\,\cot(t/2)}{2}\right)\mathrm{d}\phi \\
&= \frac{\lambda^{3/2}}{\mu}\int_0^\infty r\,\exp\left(-\frac{\lambda\pi r^2}{4}\right)\mathrm{erf}\left(\frac{r\sqrt{\lambda\pi}\,\cot(t/2)}{2}\right)\mathrm{d}r \\
&= \frac{2\lambda\cot\frac{t}{2}}{\pi\mu}\int_0^\infty \exp\left(-\frac{\lambda\pi r^2}{4\sin^2(t/2)}\right)\mathrm{d}r \\
&= \frac{2\sqrt{\lambda}\cos(t/2)}{\pi\mu} \\
&\overset{(a)}{=} \frac{1}{2}\cos\frac{t}{2},
\end{aligned} \tag{2}$$

where

$$\mathrm{erf}(x) = \frac{2}{\sqrt{\pi}}\int_0^x \mathrm{e}^{-u^2}\,\mathrm{d}u$$

is the error function and (a) follows from the fact that $\mu = 4\sqrt{\lambda}/\pi$.

The pdf of Θ on $(0, t)$ follows by differentiating (2) with respect to t, which yields

$$f_\Theta(t) = \frac{1}{4}\sin\frac{t}{2}, \quad t \in (0,\pi). \tag{3}$$

The expression for the density of Θ in $(\pi, 2\pi)$ follows by symmetry. □

https://doi.org/10.1017/jpr.2021.26 Published online by Cambridge University Press

4. The three-dimensional case

In this section, Φ is a stationary Poisson point process of intensity λ in $\mathbb{R}^3$ and $\nu(3) = 4\pi/3$ denotes the volume of the unit sphere in three dimensions.

4.1. The subset of a facet seeing a given angle

Consider a two-dimensional facet F of the Voronoi tessellation of Φ. Let X_1 and X_2 be the two nuclei creating F. Let C be the intersection point of the segment $[X_1, X_2]$ and the bisector plane P of this segment. Note that although $F \subset P$, C does not necessarily belong to F. For all $\theta \in (0, 2\pi)$, the set $\mathcal{Z}_\theta(X_1, X_2)$ of points of F that see the two nuclei X_1 and X_2 with angle θ is a random closed subset of F. Here the angle is measured in the plane that contains X_1, X_2, and Z. The set $\mathcal{Z}_\theta(X_1, X_2)$ is actually the intersection of facet F with the circle of center C and radius ρ in plane P, with

$$\rho := \frac{\|X_1 - X_2\|}{2}\left|\cot\frac{\theta}{2}\right|.$$

In the two-dimensional case, Corollary 1 gives a formula for the mean number of facets of the typical cell that contain a point seeing the nucleus of the typical cell and the other nucleus defining the facet, with angle θ. More precisely, if $Z_\theta(X, Y)$ is the point of the bisector line of $[X,Y]$ that sees the pair (X,Y) with angle $\theta \in (0, 2\pi)$, then this corollary says that

$$\mathbb{E}^0_\Phi\left[\sum_{X\in\Phi,\ X\neq 0} \mathbf{1}_{Z_\theta(0,X)\in\mathcal{V}_0}\right] = 2\sin^2\frac{\theta}{2}.$$

The three-dimensional analogue of the question considered in that corollary concerns the Palm expectation of the mean length, say L_θ, of the set of loci of the facets of the typical Voronoi cell that see the nucleus of this cell and the other nucleus defining the facet with angle θ. This analogue is evaluated in the following lemma.

Lemma 3. *For all $\theta \in (0, 2\pi)$, with $\theta \neq \pi$,*

$$L_\theta := \mathbb{E}^0_\Phi\left[\sum_{X\in\Phi,\ X\neq 0} l_1(\mathcal{Z}_\theta(0, X))\right] = 4\pi\left(\frac{6}{\pi\lambda}\right)^{1/3}\Gamma\left(\frac{4}{3}\right)\left|\cos\frac{\theta}{2}\right|\sin^3\frac{\theta}{2},$$

where l_1 denotes length.

Proof. By Slivnyak's theorem and Campbell's formula,

$$\begin{aligned}\mathbb{E}^0_\Phi\left[\sum_{X\in\Phi,\ X\neq 0} l_1(Z_\theta(0, X))\right] &= \mathbb{E}\left[\sum_{X\in\Phi} l_1(\mathcal{Z}_\theta((0, X), \Phi + \delta_0))\right]\\ &= \lambda\int_{x\in\mathbb{R}^3} \mathbf{1}_{x<0}\rho(x)\int_{t=0}^{2\pi} \mathbb{P}_\Phi(Z_\theta(t, (0, x), \Phi + \delta_0 + \delta_x) \in \mathcal{V}_0)\,\mathrm{d}x\,\mathrm{d}t,\end{aligned} \tag{4}$$

where $Z_\theta(t, (0, x), \Phi + \delta_0 + \delta_x)$ denotes the point of plane P that is at the intersection of the circle of center C and radius ρ in this plane and the line of this plane containing C and with

https://doi.org/10.1017/jpr.2021.26 Published online by Cambridge University Press

direction t, and $\rho(x)$ is defined as mentioned above, namely

$$\rho(x) := \frac{\|x\|}{2}\left|\cot\frac{\theta}{2}\right|.$$

The fact that $\theta \neq \pi$ was used in (4).

Now using isotropy, we obtain

$$\begin{aligned}\mathbb{E}_\Phi^0\left[\sum_{X\in\Phi,\ X\neq 0} l_1(Z_\theta(0,X))\right] &= 2\pi\lambda\int_{x\in\mathbb{R}^3}\mathbf{1}_{x<0}\rho(x)\,\mathbb{P}_\Phi(Z_\theta(0,(0,x),\Phi+\delta_0+\delta_x)\in\mathcal{V}_0)\,\mathrm{d}x\\ &= \pi\lambda\int_{x\in\mathbb{R}^3}\rho(x)\,\mathbb{P}_\Phi(Z_\theta(0,(0,x),\Phi+\delta_0+\delta_x)\in\mathcal{V}_0)\,\mathrm{d}x\\ &= \pi\lambda\int_{x\in\mathbb{R}^3}\rho(x)\exp(-\lambda\nu(3)R^3(x))\,\mathrm{d}x,\end{aligned}$$

where $R(x)$ is the distance between x and Z, namely

$$R(x) := \frac{\|x\|}{2}\frac{1}{\sin(\theta/2)}.$$

Passing to spherical coordinates, we get

$$\begin{aligned}\mathbb{E}_\Phi^0\left[\sum_{X\in\Phi,\ X\neq 0} l_1(Z_\theta(0,X))\right] &= 2\pi^2\lambda\left|\cot\frac{\theta}{2}\right|\int_{r>0}\exp\left(-\lambda\pi\frac{r^3}{6}\frac{1}{\sin^3(\theta/2)}\right)r^3\,\mathrm{d}r\\ &= 4\pi\left(\frac{6}{\pi\lambda}\right)^{1/3}\Gamma\left(\frac{4}{3}\right)\left|\cos\frac{\theta}{2}\right|\sin^3\frac{\theta}{2}.\end{aligned}$$

□

The last result was for $\theta \neq \pi$. For $\theta = \pi$, one should instead consider the point process Ξ of points that belong to some facet and that are the middle points of the segment $[X_1, X_2]$ of the Delaunay neighbors associated with this facet. The result is as follows.

Lemma 4.

$$N_\pi := \mathbb{E}_\Phi^0[\Xi(\mathcal{V}_0)] = 8.$$

Proof. By the same arguments as above, the mean number of points of the cell of 0 that see the two ordered nuclei $(0, X)$ with angle $\theta = \pi$ is

$$\begin{aligned}M_\pi &= \frac{\lambda}{2}\int_{x\in\mathbb{R}^3}\exp\left(-\lambda\nu(3)\left(\frac{\|x\|}{2}\right)^3\right)\mathrm{d}x\\ &= 2\pi\lambda\int_{r>0}\exp\left(-\lambda\pi\frac{1}{6}r^3\right)r^2\,\mathrm{d}r\\ &= 4.\end{aligned}$$

The result follows by symmetry. □

4.2. The angles seen from a line

The problem considered in Section 3 has a direct extension to three dimensions, where the question is again that of the distribution of the angle Θ at which the intersections of the x-axis

https://doi.org/10.1017/jpr.2021.26 Published online by Cambridge University Press

with the two-dimensional facets of the Voronoi tessellation of a Poisson point process in $\mathbb{R}^3$ see the two nuclei creating the facet.

Lemma 5. *The distribution of* $\Theta = \Theta(0)$ *under the Palm probability of* Υ *has the density*

$$f_\Theta(t) = \frac{3}{4}\left|\cos\frac{t}{2}\right|\sin^2\frac{t}{2}, \quad t \in (0, 2\pi).$$

Proof. By the same arguments as in the two-dimensional case, for all $t \in (0, \pi)$,

$$\mathbb{P}^0_\Upsilon(\Theta(0) \in (t, \pi)) = \frac{\lambda^2}{4\mu(3)} \int_{U_1\in\mathbb{R}^3}\int_{U_2\in\mathbb{R}^3} \exp(-\lambda\nu(3)R^3)\mathbf{1}_{2\arcsin\frac{r}{2R}\in(t,\pi)}\mathbf{1}_{Z\in[0,1]}\,\mathrm{d}U_1\,\mathrm{d}U_2,$$

with $\mu(3) = (4\pi/3)^{1/3}\Gamma(5/3)\lambda^{1/3}$ the linear intensity of two-dimensional facet crossings, $\nu(3)$ the volume of the unit sphere in three dimensions, and r, Z, and R geometrically defined as above. That is, $r = \|U_1 - U_2\|$, Z is the point where the bisector plane of the line segment $[U_1, U_2]$ intersects the x-axis, and $R = \|Z - U_1\| = \|Z - U_2\|$.

Let $U_1 = (x_1, y_1, z_1)$ and $U_2 = (x_2, y_2, z_2)$. The following stretch-rotation transformations are now used:

$$\begin{bmatrix} u_1 \\ u_2 \end{bmatrix} = \begin{bmatrix} 1 & 1 \\ -1 & 1 \end{bmatrix}\begin{bmatrix} x_1 \\ x_2 \end{bmatrix}, \quad \begin{bmatrix} u_3 \\ u_4 \end{bmatrix} = \begin{bmatrix} 1 & 1 \\ -1 & 1 \end{bmatrix}\begin{bmatrix} y_1 \\ y_2 \end{bmatrix}, \quad \begin{bmatrix} u_5 \\ u_6 \end{bmatrix} = \begin{bmatrix} 1 & 1 \\ -1 & 1 \end{bmatrix}\begin{bmatrix} z_1 \\ z_2 \end{bmatrix}.$$

This yields $\mathrm{d}x_1\,\mathrm{d}x_2\,\mathrm{d}y_1\,\mathrm{d}y_2\,\mathrm{d}z_1\,\mathrm{d}z_2 = \frac{1}{8}\,\mathrm{d}u_1\,\mathrm{d}u_2\,\mathrm{d}u_3\,\mathrm{d}u_4\,\mathrm{d}u_5\,\mathrm{d}u_6$. It follows that

$$\begin{aligned}\mathbb{P}^0_\Upsilon(\Theta(0) \in (t, \pi)) = \frac{\lambda^2}{32\mu(3)} \int_{\mathbb{R}^6} &\mathbf{1}_{\frac{1}{2}\left(u_1+\frac{u_3u_4}{u_2}+\frac{u_5u_6}{u_2}\right)\in[0,1]} \\ &\times \mathbf{1}_{2\arcsin\sqrt{\left(u_2^2+u_4^2+u_6^2\right)\Big/\left(u_2^2+u_3^2+u_4^2+u_5^2+u_6^2+\frac{u_3^2u_4^2}{u_2^2}+\frac{u_5^2u_6^2}{u_2^2}+\frac{2u_3u_4u_5u_6}{u_2^2}\right)}\in(t,\pi)} \\ &\times \mathrm{e}^{-\frac{A}{8}\left(u_2^2+u_3^2+u_4^2+u_5^2+u_6^2+\frac{u_3^2u_4^2}{u_2^2}+\frac{u_5^2u_6^2}{u_2^2}+\frac{2u_3u_4u_5u_6}{u_2^2}\right)^{3/2}} \,\mathrm{d}u_1\,\mathrm{d}u_2\,\mathrm{d}u_3\,\mathrm{d}u_4\,\mathrm{d}u_5\,\mathrm{d}u_6,\end{aligned}$$

where $A = 4\pi\lambda/3$. Now the first indicator function can be eliminated by carrying out the integration over u_1, where the condition for the first indicator function is met when

$$0 \le \frac{1}{2}\left(u_1 + \frac{u_3u_4}{u_2} + \frac{u_5u_6}{u_2}\right) \le 1,$$

or equivalently when

$$-\frac{u_3u_4}{u_2} - \frac{u_5u_6}{u_2} \le u_1 \le 2 - \frac{u_3u_4}{u_2} - \frac{u_5u_6}{u_2}.$$

This yields a factor of two.

Spherical coordinates, i.e. $(u_2, u_4, u_6) = (r\sin\psi\cos\varphi, r\sin\psi\sin\varphi, r\cos\psi)$, and polar coordinates, i.e. $(u_3, u_5) = (\rho\cos\phi, \rho\sin\phi)$, are now used to handle the second indicator function:

$$\begin{aligned}\mathbb{P}^0_\Upsilon(\Theta(0) \in (t, \pi)) = \frac{\lambda^2}{16\mu(3)} &\int_0^{2\pi}\mathrm{d}\varphi\int_0^{\pi}\sin\psi\,\mathrm{d}\psi\int_0^{2\pi}\mathrm{d}\phi\int_0^{\infty} r^2\,\mathrm{d}r \\ &\times \int_0^{\infty}\rho\mathbf{1}_{2\arcsin\frac{r}{\sqrt{r^2+a^2(\psi,\varphi,\phi)\rho^2}}\in(t,\pi)} \\ &\times \mathrm{e}^{-\frac{A}{8}(r^2+a^2(\psi,\varphi,\phi)\rho^2)^{3/2}}\,\mathrm{d}\rho, \end{aligned} \tag{5}$$

https://doi.org/10.1017/jpr.2021.26 Published online by Cambridge University Press

where

$$a^2(\psi, \varphi, \phi) = \frac{1 - (\sin\psi \sin\phi \sin\varphi - \cos\psi \cos\phi)^2}{\sin^2\psi \cos^2\varphi}.$$

The next step is to carry out the integration with respect to ρ. The indicator function in question is equal to one on an interval with left limit $\rho^- = 0$ (the argument of the arcsine is one, so $\pi > t$ is true as $t \in (0, \pi)$) and with the right limit obtained by solving

$$\frac{r^2}{r^2 + a^2(\psi, \varphi, \phi)\rho^2} = \sin^2\frac{t}{2},$$

namely $\rho^+ = (r/a)\cot(t/2)$. Hence we can write the integrals with respect to ρ and r in (5) as

$$\int_0^\infty r^2\,\mathrm{d}r \int_0^{(r/a)\cot(t/2)} \rho\, \mathrm{e}^{-\frac{A}{8}(a^2\rho^2 + r^2)^{3/2}}\,\mathrm{d}\rho = \frac{32\,\Gamma(5/3)}{9a^2A^{5/3}}\left(1 - \sin^3\frac{t}{2}\right).$$

Thus the final step involves calculating the angular integrals as

$$\begin{aligned}
\mathbb{P}^0_\Upsilon(\Theta(0) \in (t, \pi)) &= \frac{2\,\Gamma(5/3)\lambda^2}{9\,A^{5/3}\mu(3)}\left(1 - \sin^3\frac{t}{2}\right)\int_0^{2\pi}\mathrm{d}\varphi \int_0^\pi \sin\psi\,\mathrm{d}\psi \int_0^{2\pi}\frac{1}{a^2(\psi, \varphi, \phi)}\,\mathrm{d}\phi \\
&= \frac{2\,\Gamma(5/3)\lambda^2}{9\,A^{5/3}\mu(3)}\left(1 - \sin^3\frac{t}{2}\right)\int_0^{2\pi}\mathrm{d}\varphi \int_0^\pi \sin\psi\,\mathrm{d}\psi \\
&\quad \times \int_0^{2\pi}\frac{\sin^2\psi\cos^2\varphi}{1 - (\sin\psi\sin\phi\sin\varphi - \cos\psi\cos\phi)^2}\,\mathrm{d}\phi \\
&= \frac{4\pi\,\Gamma(5/3)\lambda^2}{9\,A^{5/3}\mu(3)}\left(1 - \sin^3\frac{t}{2}\right)\int_0^{2\pi}|\cos\varphi|\,\mathrm{d}\varphi \int_0^\pi \sin^2\psi\,\mathrm{d}\psi \\
&\overset{\text{(a)}}{=} \frac{1}{2}\left(\frac{4\pi}{3}\right)^{1/3}\frac{\Gamma(5/3)\lambda^{1/3}}{\mu(3)}\left(1 - \sin^3\frac{t}{2}\right) \\
&= \frac{1}{2}\left(1 - \sin^3\frac{t}{2}\right), \qquad (6)
\end{aligned}$$

where the formula $\mu(3) = (4\pi/3)^{1/3}\Gamma(5/3)\lambda^{1/3}$ was used, and in (a) we used $A = 4\pi\lambda/3$.

The distribution of Θ follows by differentiating (6) with respect to t, which yields

$$f_\Theta(t) = \frac{3}{4}\cos\frac{t}{2}\sin^2\frac{t}{2}, \quad t \in (0, \pi).$$

The expression for density of Θ follows from the symmetry and is given as

$$f_\Theta(t) = \frac{3}{4}\left|\cos\frac{t}{2}\right|\sin^2\frac{t}{2}, \quad t \in (0, 2\pi). \qquad \square$$

Note that the density is zero at $t = \pi$.

https://doi.org/10.1017/jpr.2021.26 Published online by Cambridge University Press

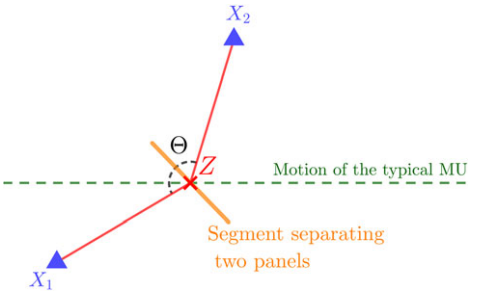


FIGURE 4. Panel swap with two panels.

5. Cellular networking motivations

Consider a cellular radio network where a mobile user (MU) connects to the nearest base station. If the locations of the base stations are some realization of a stationary point process, the service region of each base station is essentially the Voronoi cell of this base station [2]. A mobile user moving on a straight line crosses cell boundaries of the Voronoi tessellation, where it performs *inter-cell handovers* [5] that involve the transfer of the cellular connection between the two base stations sharing the cell boundary. When the mobile user handset is equipped with two-directional panels, the handset might have to swap panels depending on whether or not the two base stations involved in the inter-cell handover are seen by the same panel. Whether a panel swap occurs hence depends on the angle at which the mobile user at the cell boundary sees the two base stations sharing the boundary. The evaluation of the frequency of panel swaps at handover times requires evaluating the distribution of the angle with which the intersection point of a randomly oriented line and the Voronoi facet sees the two nuclei that define the facet.

Assume that the base stations of a cellular radio network are located at positions that are a realization of a Poisson point process Φ of intensity λ in the plane, as illustrated in Figure 2. (The Poisson assumption is common in the wireless network modeling literature [2,3,5,6].) The dashed straight line represents the path of a mobile user, which is assumed to be along the x-axis without loss of generality. A 'cross' in the figure denotes a point at the intersection of a Voronoi facet and the line of motion of the mobile user. These points are those where the mobile user has to perform inter-cell handovers.

The situation motivating the previous analysis is that where the mobile user is equipped with *directional panels*. The simplest situation is that where the mobile user has two panels, one creating a beam covering the angular regions $[\chi, \chi + \pi)$, and the other a beam covering the region $[\chi + \pi, \chi + 2\pi)$, where χ is uniformly distributed on $[0, \pi]$. When the mobile user reaches an inter-cell handover point, two things may happen. If the two base stations involved in the handover are not on the same side of the line with angle χ (i.e. they are in the beams of different panels, as depicted in Figure 4), there is a *panel swap*, which has a certain overhead cost. If the base stations are on the same side of this line, there is no panel swap (see an instance of this case in Figure 5), and no overhead cost is incurred by the mobile user. In this context, it is important to evaluate the ergodic fraction of inter-cell handovers that involve such a panel swap.

A more general situation is that where there are 2^m panels with $m \geq 1$, each surveying an angle (or beam) of the form $[\chi + 2k\pi/2^m, \chi + 2(k+1)\pi/2^m)$, $k = 0, 1, \ldots, 2^m - 1$. Here too, the main question is again about the fraction of inter-cell handovers that involve a panel swap

https://doi.org/10.1017/jpr.2021.26 Published online by Cambridge University Press

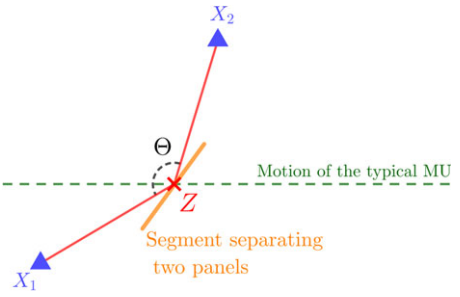


FIGURE 5. No panel swap with two panels.

(which happens when the two base stations are seen by the mobile user within different panel beams). This question is answered in the next corollary of Lemma 2.

Corollary 3. *When the typical mobile user has 2^m panels, $m \geq 1$, the probability p of a panel swap at the user during an inter-cell handover is*

$$p = \frac{2^m}{\pi} \sin \frac{\pi}{2^m}, \quad m \geq 1.$$

Proof. The case of two panels, i.e. $m = 1$, is considered first. Without loss of generality, the coordinate system can be taken such that the inter-cell handover point is the origin O. Let X denote the minimal Delaunay neighbor, $A(X)$ its angle, and Θ the angle with which O sees the two Delaunay neighbors, with the foregoing conventions.

As Figures 4 and 5 show, a panel swap occurs if and only if one of the two ends of the segment separating two panels is 'within' the angle Θ. More precisely, let χ denote the angle of that segment, which is uniformly distributed on $(0, \pi)$. If $\Theta \in (0, \pi)$, there is a panel swap if and only if either $\chi \in (A(X), A(X) + \Theta)$ or $\chi + \pi \in (A(X), A(X) + \Theta)$, and these two events cannot simultaneously hold. Similarly, if $\Theta \in (\pi, 2\pi)$, there is a panel swap if and only if either $\chi \in (A(X) + \Theta, A(X))$ or $\chi + \pi \in (A(X) + \Theta, A(X))$, with these two events excluding each other. Since Θ, $A(X)$, and χ are independent, the probability of a panel swap is

$$\begin{aligned} p &= \int_0^{\pi} f_{\Theta}(t) \frac{1}{2\pi} \left(\int_0^t \mathrm{d}u + \int_0^t \mathrm{d}u \right) \mathrm{d}t + \int_{\pi}^{2\pi} f_{\Theta}(t) \frac{1}{2\pi} \left(\int_0^{2\pi - t} \mathrm{d}u + \int_0^{2\pi - t} \mathrm{d}u \right) \mathrm{d}t \\ &= \frac{1}{2\pi} \int_0^{\pi} t \sin \frac{t}{2} \, \mathrm{d}t \\ &= \frac{2}{\pi}, \end{aligned}$$

where the expression obtained in (3) was used.

This can be generalized to the case where the mobile user has 2^m panels, with $m \geq 1$.

Using the same notation as above, if $\Theta \in (0, \pi)$, a panel swap occurs if and only if there is at least one $k = 0, 1, \ldots, 2^m - 1$ such that

$$\chi + \frac{2k\pi}{2^m} \in (A(X), A(X) + \Theta). \tag{7}$$

If $\Theta \in (\pi, 2\pi)$, a panel swap occurs if and only if

$$\chi + \frac{2k\pi}{2^m} \in (A(X) + \Theta, A(X)), \tag{8}$$

https://doi.org/10.1017/jpr.2021.26 Published online by Cambridge University Press

for some $k = 0, 1, \ldots, 2^m - 1$. Hence a panel swap is certain if $\Theta \in (\pi/2^{m-1}, 2\pi - \pi/2^{m-1})$. The cases $\Theta \in (0, \pi/2^{m-1})$ and $\Theta \in (2\pi - \pi/2^{m-1}, 2\pi)$ are symmetric. For $\Theta \in (0, \pi/2^{m-1})$ (respectively $\Theta \in (2\pi - \pi/2^{m-1}, 2\pi)$), there are 2^m symmetric possibilities for a panel swap, one for each value of $k = 0, 1, \ldots, 2^m - 1$ in equation (7) (respectively (8)). These events are disjoint and have the same probability. Since Θ, $A(X)$, and χ are independent, the probability of a panel swap is hence

$$\begin{aligned} p &= \frac{2^{m+1}}{2\pi} \int_0^{\pi/2^{m-1}} f_\Theta(t)\,\mathrm{d}t \int_0^t \mathrm{d}u + \int_{\pi/2^{m-1}}^{2\pi-\pi/2^{m-1}} f_\Theta(t)\,\mathrm{d}t \\ &= \frac{2^m}{4\pi} \int_0^{\pi/2^{m-1}} t \sin\frac{t}{2}\,\mathrm{d}t + \frac{1}{4}\int_{\pi/2^{m-1}}^{2\pi-\pi/2^{m-1}} \sin\frac{t}{2}\,\mathrm{d}t \\ &= \frac{2^m}{\pi}[\sin t - t\cos t]_0^{\pi/2^m} + \cos\frac{\pi}{2^m} \\ &= \frac{2^m}{\pi}\sin\frac{\pi}{2^m} - \cos\frac{\pi}{2^m} + \cos\frac{\pi}{2^m} \\ &= \frac{2^m}{\pi}\sin\frac{\pi}{2^m}. \end{aligned}$$

□

6. Possible extensions

It would be interesting to extend the analysis to dimensions higher than three. Another practically useful line of research would be the extension of this type of analysis to Voronoi tessellations associated with more versatile parametric classes of stationary point processes, for instance determinantal or permanantal.

Acknowledgements

This work was supported by the ERC NEMO grant, under the European Union's Horizon 2020 research and innovation programme, grant agreement no. 788851 to INRIA. The authors thank F. Abinader and L. Uzeda-Garcia of Bell Laboratories for the discussions that led to the formulation of the problem. They also thank D. Stoyan, J. Møller, and M. Haenggi for their comments on the topic discussed in this note.

References

[1] Aldous, D. and Lyons, R. 2007. Processes on unimodular random networks. *Electron. J. Prob.* **12**, 1454–1508.

[2] Andrews, J. G., Baccelli, F. and Ganti, R. K. 2011. A tractable approach to coverage and rate in cellular networks. *IEEE Trans. Commun.* **59**, 3122–3134.

[3] Baccelli, F. and Błaszczyszyn, B. 2009. *Stochastic Geometry and Wireless Networks,* vol. I, *Theory* (Foundations and Trends in Networking). Now Publishers.

[4] Baccelli, F. and Brémaud, P. 2003. *Elements of Queueing Theory: Palm Martingale Calculus and Stochastic Recurrences* (Applications of Mathematics: Stochastic Modelling and Applied Probability **26**). Springer.

[5] Baccelli, F. and Zuyev, S. 1996. Stochastic geometry models of mobile communication networks. In *Frontiers in Queueing: Models and Applications in Science and Engineering*, ed. J. Dshalalow, Chapter 8, pp. 227–243. CRC Press.

[6] Kalamkar, S. S., Baccelli, F., Abinader Jr, F. M., Marcano Fani, A. S. and Uzeda Garcia, L. G. 2020. Beam management in 5G: a stochastic geometry analysis. To appear in *IEEE Trans. Wireless Commun.* Available at https://arxiv.org/abs/2012.03181.

[7] Møller, J. 1989. Random tessellations in $\mathbb{R}^d$. *Adv. Appl. Prob.* **21**, 37–73.

[8] Muche, L and Stoyan, D. 1992. Contact and chord length distributions of the Poisson Voronoi tessellation. *J. Appl. Prob.* **29**, 467–471.

https://doi.org/10.1017/jpr.2021.26 Published online by Cambridge University Press